

## Critical Exponents at the Ferromagnetic Transition in Tetrakis(dimethylamino)ethylene-C<sub>60</sub> (TDAE-C<sub>60</sub>)

Aleš Omerzu,<sup>1,2</sup> Madoka Tokumoto,<sup>2</sup> Bosiljka Tadić,<sup>1</sup> Dragan Mihailovic<sup>1</sup>

<sup>1</sup>*Jožef Stefan Institute, Jamova 39, 1000 Ljubljana, Slovenia*

<sup>2</sup>*Nanotechnology Research Institute, National Institute of Advanced Industrial Science and Technology (AIST), 1-1-1 Umezono, Tsukuba, Ibaraki 305-8568, Japan*

(Received 13 February 2001; published 5 October 2001)

Critical exponents at the ferromagnetic transition were measured for the first time in an organic ferromagnetic material tetrakis(dimethylamino)ethylene fullerene[60] (TDAE-C<sub>60</sub>). From a complete magnetization-temperature-field data set near  $T_c = 16.1 \pm 0.05$ , we determine the susceptibility and magnetization critical exponents  $\gamma = 1.22 \pm 0.02$  and  $\beta = 0.75 \pm 0.03$ , respectively, and the field vs magnetization exponent at  $T_c$  of  $\delta = 2.28 \pm 0.14$ . Hyperscaling is found to be violated by  $\Omega \equiv d' - d \approx -1/4$ , suggesting that the onset of ferromagnetism can be related to percolation of a particular contact configuration of C<sub>60</sub> molecular orientations.

DOI: 10.1103/PhysRevLett.87.177205

PACS numbers: 75.50.Xx

Molecular ferromagnetism, particularly when only electrons in  $p$  orbitals are involved in the magnetic interactions, is a relatively newly discovered phenomenon. Of the few compounds discovered thus far which display signatures of proper ferromagnetic (FM) behavior [1,2], the most studied has been tetrakis(dimethylamino)ethylene fullerene[60] (TDAE-C<sub>60</sub>), which—by virtue of its relatively simple synthesis (at least in powder form) and high Curie temperature of  $T_c = 16$  K—has been investigated by many groups. However, the magnetic properties of this material are not straightforward, and measurements on powder samples have led to apparently conflicting proposals regarding its low-temperature state ranging from superparamagnetism [3] to spin glass [4] as well as ferromagnetism. More recently, low-field electron paramagnetic resonance [5] and susceptibility measurements on high-quality single crystals showed more conclusively that the material—if properly chemically and thermally prepared [6]—displays clear signs of a transition to a ferromagnetic state at around 16 K, in agreement with the original suggestion of its discoverers [1].

The origin of the ferromagnetic exchange interaction between C<sub>60</sub> molecules in TDAE-C<sub>60</sub> has been studied theoretically by a number of groups [6–8]. Recently, it was discovered [6] that in the FM  $\alpha$  phase of TDAE-C<sub>60</sub> two different orientations of C<sub>60</sub> molecules may occur at low temperatures (labeled I and II). These orientations can lead to different contact C<sub>60</sub> configurations along the direction of closest contact ( $c$  axis) [6], which profoundly affect the exchange interaction along the  $c$  axis [7]. In the nonmagnetic  $\alpha'$  phase, the 6-6 double bond (nearly) faces the center of the hexagon on the neighboring molecule, whereas, in the FM phase, a number of additional different mutual orientations are possible. But, among these, the alternating I-II contact configuration—in which the double bond on one molecule approximately faces the center of the pentagon of its neighbor—was shown to be dominant in the ferromagnetic state.

To confirm the observation of a proper FM state and investigate the associated critical behavior, we report here the first measurements of the critical exponents associated with the ferromagnetic transition of TDAE-C<sub>60</sub>. The measurements, which are also the first for any organic system, are found to give remarkably self-consistent values of the critical exponents in agreement with behavior expected for a ferromagnetic transition in a system with a certain degree of disorder. They confirm the essentially FM behavior, and also give important insight into the interactions responsible for the ferromagnetism in these unusual materials.

Single crystals of TDAE-C<sub>60</sub> were grown by a diffusion method as described in [9]. For magnetic measurements, a number of crystals from different growth batches were sealed into quartz tubes under helium. Since the “as grown” crystals of TDAE-C<sub>60</sub> are in their  $\alpha'$  modification which shows no low-temperature ferromagnetic transition [10], they were annealed in order to transform them into the ferromagnetic  $\alpha$  modification. The annealing was carefully done through several intervals of 1 h at 70 °C, each of them followed by a measurement of the low-temperature magnetic properties. The annealing procedure was stopped at the point where the low-temperature saturation magnetization of the crystals reached its maximum, i.e., when the whole sample had transformed into the  $\alpha$  modification. Magnetic measurements were performed with a Quantum Design MPMS SQUID magnetometer which enables a temperature stability better than 10 mK and a measurement of magnetization with a relative error of less than 0.1% and, since the magnetic response for crystals smaller than 3 mm across is pointlike, the problems associated with demagnetization factors are avoided. Furthermore, the magnetization was found to be independent of orientation.

In order to determine accurately the critical temperature of the ferromagnetic transition,  $T_c$ , and the critical exponent  $\gamma$  which defines the temperature dependence of the zero-field magnetic susceptibility  $\chi$  in the critical region just above the transition  $\chi(T) \sim (T/T_c - 1)^{-\gamma}$ , we have

measured the static magnetic susceptibility in a temperature interval 16–17.6 K.  $\chi$  was determined as a slope of the magnetization versus field curve  $M(H)$ , through ten equidistant points between  $-5$  and  $5$  Oe every 50 mK. To determine  $T_c$  and  $\gamma$  from the experimental results, we plot the inverse logarithmic derivative  $(d \ln \chi / dT)^{-1} \sim -(T/T_c - 1)/\gamma$  versus reduced temperature  $\epsilon \equiv (T - T_c)/T_c$ . By varying  $T_c$ , the data are made to appear on a straight line pointing to the origin. The best fit of the data is shown in Fig. 1a for  $T_c = 16.05$ . From the slope we determine the exponent as  $\gamma = 1.22 \pm 0.02$ , the error reflecting variations in  $T_c$  within the range 16.05–16.15 where the accuracy of fit cannot be further improved.

The critical exponent  $\beta$  describes the temperature dependence of the spontaneous magnetization,  $M_S$ , in the critical region  $T \lesssim T_c$  through the relation  $M_S \sim \mathcal{B}(1 - T/T_c)^\beta$ . To determine  $\beta$ , we have measured the magnetization at temperatures between 14.4 and 16 K in a low magnetic field. The data are shown in Fig. 1b for 20 Oe. In fact, the *functional form* of the temperature dependence of the magnetization at low fields and the temperature range 15.6–16.1 K does not depend on the value of the field. In this temperature range and for small  $H$ , different isotherms appear to be straight lines on a  $\log H$ - $\log M$  plot (see Fig. 2). This implies that different  $M(T)$  curves can be scaled to a unique functional form as Fig. 1b shows. The scaled values of magnetization vs temperature for lowest measured field  $H = 1$  Oe are seen to coincide with the ones measured at 20 Oe near  $T_c$ . In addition, the extrapolations [11] of the power-law isotherms in Fig. 2 to the  $H = 0$  axis leads to the same  $T$  dependence of the spontaneous magnetization near the critical temperature, as is suggested by the susceptibility measurements. Fitting the

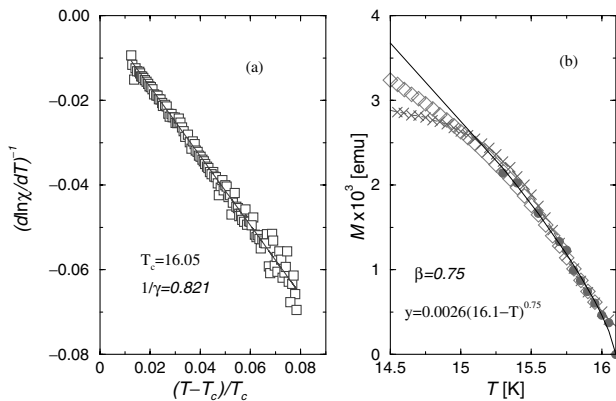


FIG. 1. (a) Inverse logarithmic derivative of the static susceptibility of TDAE-C<sub>60</sub>,  $[d(\ln \chi)/dT]^{-1} \sim -(T/T_c - 1)/\gamma$  plotted against reduced temperature  $(T - T_c)/T_c$  in the critical region above  $T_c$ . (b) Temperature dependence of the magnetization of TDAE-C<sub>60</sub> measured in a static magnetic field of 20 Oe (open symbols) for temperatures below  $T_c$ . Also shown are values of the magnetization measured at a field of 1 Oe (crosses) scaled by a factor of 4.75 and extrapolated values for zero field (bullets) scaled by factor of 6 along the vertical axis. Solid line: The curve fit to  $y = \mathcal{B}(T_c - T)^\beta$ , as indicated.

magnetization curve to the expected power-law behavior, we find the best fit with  $T_c = 16.1$  of  $\beta = 0.75$  within statistical error bars of 0.03 (cf. Fig. 1b).

At  $T = T_c$  the field dependence of magnetization follows the critical isotherm  $H \sim M^\delta$ , where  $\delta$  is the exponent for the critical isotherm. To determine the critical exponent  $\delta$  we have measured the magnetization over four decades of magnetic fields between 1 Oe and 10 kOe at several temperatures above and below  $T_c$ , as shown in Fig. 2. By fitting several isotherms near the  $T_c$  values suggested above, we find the exponent  $\delta$  in the range  $\delta = 2.14$ – $2.41$ , the uncertainty reflecting the chosen value of  $T_c$ , giving  $\delta = 2.28 \pm 0.14$ .

An important feature of the measurements is that the exponents  $\gamma$ ,  $\beta$ , and  $\delta$  do not obey the scaling relation  $\gamma = \beta(\delta - 1)$ , which is expected to apply at a second-order phase transition for a nondisordered system in equilibrium. Before we discuss the possible origin of the scaling violation, we show—as an independent test of the consistency of the values for the critical exponents—that the measured data obey a general scaling form [12,13],

$$M(T, H) \sim H^{1/\delta} M(\epsilon/H^{1/\beta\delta}, 1), \quad (1)$$

in the critical region at low fields  $H \rightarrow 0$  and small relative temperatures  $\epsilon \equiv (T - T_c)/T_c \rightarrow 0$ . Equation (1) follows directly from the statement that the singular part

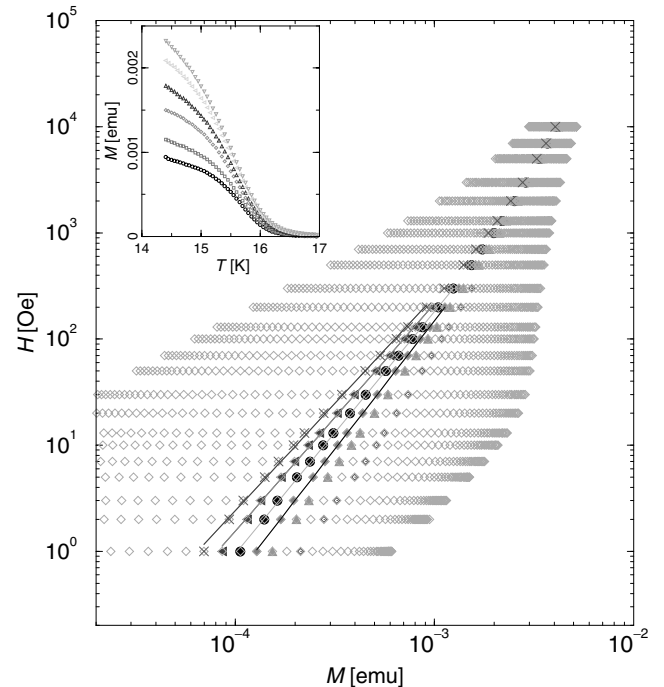


FIG. 2. Field dependence of magnetization for different temperatures in the range from 14.4 to 17.6 K (plotted right to left) every 0.05 K. Emphasized are several isotherms near  $T_c$ , in particular, for  $T = 16.1, 16.05, 16, 15.95,$  and  $15.9$  K with the corresponding fit lines for low field values also shown, their slopes giving the critical exponent  $\delta$ . The axes are cut off to reflect the uncertainty in the measurements. Inset: Magnetization vs temperature data for field values  $H = 2, 3, 5, 7, 10,$  and  $13$  Oe.

of a thermodynamic potential (or, equivalently, its derivatives) is a generalized homogeneous function of its arguments. That is,  $M(b^{\lambda_T} \epsilon, b^{\lambda_H} H) = b^\lambda M(\epsilon, H)$ , by taking  $b^{\lambda_H} H \sim 1$  and the standard identification of the scaling exponents in terms of  $\beta$  and  $\delta$  (see [12,13]). In Fig. 3 we plot  $M/H^{1/\delta}$  vs  $x \equiv \epsilon/H^{1/\beta\delta}$  using the values of the critical exponents determined above and  $T_c = 16.1$ . The consistency in the exponents is demonstrated by a “parallel” collapse of the curves for different  $H$  values. As discussed in Ref. [13], the characteristic scaling function  $M/H^{1/\delta} \equiv m(x)$  with respect to  $x$  alone cannot be determined directly by this fit, since neither argument of  $M(x, 1)$  on the right-hand side of Eq. (1) is small in the critical region. Following the procedure discussed in Ref. [13], we determine the *characteristic scaling function* by plotting the reduced data  $m(x)/m(0)$  vs  $x/x_0$ , where  $x_0$  are the values of the argument where deviations from power-law behavior start to occur [related to the amplitude  $\mathcal{B}$  in the  $M(T)$  curve in Fig. 1b]. The resulting plot of the data is shown in Fig. 3b. The scaling plot confirms both the consistency of the measured critical exponents within the quoted error bars and determines the scaling function of the phase transition.

A complete list of the critical exponents at the ferromagnetic transition in TDAE-C<sub>60</sub> is given in Table I. From previous measurements [5] of single crystals it appears that TDAE-C<sub>60</sub> for  $10 \lesssim T < 16$  K is a ferromagnet with localized magnetic moments with a very low anisotropy. Therefore, we first discuss our results in comparison with the isotropic three-dimensional Heisenberg model. The theoretical values calculated with the renormalization group (RG) techniques [14] for a Heisenberg model with spins  $S = 1/2$  and nearest-neighbor interactions are also shown in Table I. It is clear that the mea-

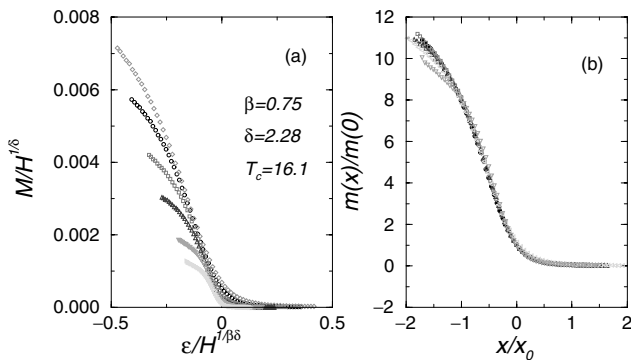


FIG. 3. (a) Scaling collapse according to Eq. (1) of the magnetization vs temperature curves for several values of the field  $H = 2, 3, 5, 7, 10,$  and  $13$  Oe, which are shown in the inset of Fig. 2.  $\epsilon \equiv (T - T_c)/T_c$  with  $T_c = 16.1$  and values of the exponents  $\beta = 0.75$  and  $\delta = 2.28$  are used in the fit. The deviations from the master curve behavior for different  $H$  values indicate a crossover value  $x_0$  of  $x \equiv \epsilon/H^{1/\beta\delta}$ , where the two variables in Eq. (1) become comparable. (b) The characteristic scaling function  $m(x)/m(0)$  vs  $x/x_0$  computed from data shown in (a) as a function of the variable  $x$ .

TABLE I. Complete list of critical exponents at the ferromagnetic transition in TDAE-C<sub>60</sub>.

Syst.	$\gamma$	$\beta$	$\delta$	$\nu$	$\alpha$	$\Omega$	$\bar{\beta}$
TDAE <sup>a</sup>	1.22	0.75	2.28	1.06	-0.72	-0.26	1.01
RP <sup>b</sup>	1.82	0.41	5.43	0.88	...	-0.66	0.99
RFIM <sup>c</sup>	1.9	0.06	?	1.02	-0.02	-1	1.06
REIM <sup>d</sup>	1.34	0.35	4.78	0.68	-0.05	0	...
PHM <sup>e</sup>	1.38	0.36	4.80	0.70	-0.12	0	...

<sup>a</sup>Numerical values of the critical exponents of TDAE-C<sub>60</sub>: measured in this work  $\gamma$ ,  $\beta$ , and  $\delta$ , and the remaining exponents are computed via valid scaling relations, as explained in the text.  $\Omega$  represents effective dimensional reduction in the hyperscaling relation.

<sup>b</sup>Exponents of random percolation, Ref. [15]. Here  $\Omega$  and  $\bar{\beta}$  are the exponents related to the backbone percolation.

<sup>c</sup>Critical exponents for the random-field Ising model from first reference in [16].

<sup>d</sup>Exponents for the random-exchange Ising model from Ref. [17].

<sup>e</sup>Exponents for pure Heisenberg model, from Ref. [14], all for spatial dimension  $d = 3$ .

sured exponents differ significantly from the ones of the 3D Heisenberg model. In addition, violation of the scaling relation, i.e.,  $\gamma \neq \beta(\delta - 1)$ , indicates an entirely different nature of the transition in TDAE-C<sub>60</sub>. In particular, an additional exponent  $\bar{\gamma} \equiv \beta(\delta - 1)$  can be defined, which in turn violates the hyperscaling relation [16] by an amount  $\Omega$ . A modified hyperscaling relation then holds:

$$2\beta + \gamma = (d + \Omega)\nu, \quad (2)$$

where  $d = 3$  is spatial dimension of the system and  $\nu$  is the correlation length exponent. Physical insight of the relation (2) can be achieved by considering another exponent  $\bar{\beta}$  defined by [18]

$$\bar{\beta}/\nu = \beta/\nu - \Omega, \quad (3)$$

such that, together with  $\bar{\gamma}/\nu = \gamma/\nu + \Omega$ , the original hyperscaling relation is satisfied, i.e.,  $2\bar{\beta} + \bar{\gamma} = d\nu$ . From the known  $\bar{\gamma} = 0.96$  we find  $\Omega\nu = -0.26$  and thus  $\bar{\beta} = 1.01$ . This immediately gives  $\nu = (2\bar{\beta} + \bar{\gamma})/3 = 0.99$ . Therefore,  $\Omega = -0.26 < 0$ , meaning that the effective dimension  $d' \equiv d + \Omega$  in Eq. (2) is reduced by  $\sim 1/4$ , within the error bars of the measurements. A reduced effective dimension indicates that the fluctuations at the transition are stronger than purely thermal fluctuations, as, for instance, an enhancement of fluctuations due to configurational disorder in random-field systems [19]. Within the random-field Ising model, the dimensional reduction for  $d = 3$  was estimated to lie between  $\Omega = -1$  and  $\Omega = -1.5$  [16]. The origin of disorder in TDAE-C<sub>60</sub> can indeed be related to random spatial realizations of the contact configurations of C<sub>60</sub> molecular orientations. As discussed in Ref. [6], only the configuration with alternating I-II orientations along the  $c$  axis is compatible with ferromagnetism, but other contact configurations may also occur with a finite probability. Therefore, it is quite plausible that the long-range ferromagnetic order

sets in when a percolating cluster of the “right” contact configurations is established. Indeed, the value of the exponent  $\bar{\beta} \approx 1$  is quite compatible with the backbone percolation [15] of a random incipient cluster.

Beside the measured exponents  $\beta$ ,  $\gamma$ , and  $\delta$  in Table I we have computed the rest of the exponents using the valid scaling relations. Of course, direct measurements of the exponents  $\nu$ ,  $\gamma$ ,  $\eta$ , e.g., by scattering experiments [20], and measurements of the specific heat exponent  $\alpha$  in TDAE-C<sub>60</sub> are necessary in order to independently confirm the accuracy of these values. Preliminary measurements in fact suggest that no anomaly occurs in the specific heat [21], in agreement with the predicted  $\alpha < 0$ . Also, for comparison, in Table I we have quoted the accepted values of the exponents for random-field Ising systems as well as for the case of a random-exchange (or diluted) Ising model [17], in which disorder of the kind expected here is a relevant perturbation at the phase transition. At this point, we wish to emphasize the distinction between the microscopic origin of the FM interaction between C<sub>60</sub> molecules and the fluctuation mechanisms leading to collective ferromagnetic behavior. The global response studied here does not allow us to make detailed conclusions about the microscopic picture, for which local microscopic probes such as ESR [8] and x-ray structure [6] are more appropriate.

In conclusion, the excellent reproducibility of the measured exponents in different crystals and over time strongly suggests that the exponents are intrinsic to the material. Violation of the hyperscaling relation that implies an effective dimensional reduction by approximately a quarter ( $d' \approx d - 1/4$ ) indicates that additional degrees of freedom—rotation of the C<sub>60</sub> molecules—significantly alters the nature of the ferromagnetic phase transition in TDAE-C<sub>60</sub>. The transition appears to be in a new universality class which shares some similarity with a backbone percolation and is attributed to the presence of disorder in the C<sub>60</sub> molecular orientations near the transition temperature.

This work was supported by the Ministry of Education, Science and Sport of the Republic of Slovenia. The authors wish to acknowledge the ESF MOLMAG program.

- 
- [1] P.-M. Allemand *et al.*, *Science* **253**, 301 (1991).  
 [2] A. Mrzel *et al.*, *Chem. Phys. Lett.* **298**, 329 (1998).  
 [3] K. Tanaka *et al.*, *Phys. Rev. B* **47**, 7554 (1993).  
 [4] P. Venturini *et al.*, *Int. J. Mod. Phys. B* **6**, 3947 (1992).

- [5] D. Arcon, P. Cevc, A. Omerzu, and R. Blinc, *Phys. Rev. Lett.* **80**, 1529 (1998).  
 [6] B. Narymbetov *et al.*, *Nature (London)* **407**, 883 (2000).  
 [7] See, for example, T. Sato, T. Yamabe, and K. Tanaka, *Phys. Rev. B* **56**, 307 (1997), and references therein.  
 [8] K. Mizoguchi, M. Machino, H. Sakamoto, M. Tokumoto, T. Kawamoto, A. Omerzu, and M. Mihailovic, *Synth. Met.* (to be published); *Phys. Rev. B* **63**, 140417(R) (2001).  
 [9] B. Narymbetov, H. Kobayashi, M. Tokumoto, A. Omerzu, and D. Mihailovic, *Chem. Commun. (Cambridge)* **16**, 1511 (1999).  
 [10] A. Omerzu, D. Mihailovic, and M. Tokumoto, *Phys. Rev. B* **61**, R11883 (2000).  
 [11] The extrapolation is reliable for small deviations of temperature from  $T_c$ , where various curves are linear in a double-logarithmic plot.  
 [12] H. E. Stanley, *Introduction to Phase Transition and Critical Phenomena* (Oxford University, London, 1971).  
 [13] S. Milošević and H. E. Stanley, *Phys. Rev. B* **5**, 2526 (1972). Notice that in this paper  $H(T, M)$  was considered.  
 [14] L. C. Le Guillou and J. Zinn-Justin, *Phys. Rev. B* **21**, 3976 (1980).  
 [15] G. Grimmett, *Percolation* (Springer-Verlag, Berlin, 1999), 2nd ed.  
 [16] Hyperscaling violation has been studied in relation to ferromagnetic phase transition in the random-field Ising model, where an additional exponent  $\tilde{\gamma} \equiv \gamma - \Omega$  governs behavior of the disconnected susceptibility  $\chi_{\text{dis}} \sim [\langle S \rangle^2] - [\langle S \rangle]^2$ . The averages  $\langle \dots \rangle$  and  $[\dots]$  are over thermal and configurational fluctuations, respectively. See M. E. J. Newman and G. T. Barkema, *Phys. Rev. E* **53**, 393 (1996); J. C. Le Guillou, cond-mat/9706254.  
 [17] H. G. Ballesteros, L. A. Fernández, V. Martín-Mayor, and A. Muñoz Sudupe, *Phys. Rev. B* **58**, 2740 (1998).  
 [18] For dynamic phase transitions, the new exponent  $\bar{\beta}$  is related to an underlying dynamic process, with the survival probability at long times  $t \rightarrow \infty$  given by  $P \sim T^{-\bar{\beta}/\nu}$ . Several examples of dynamic phase transitions with violation of hyperscaling have been studied thus far. See, for instance, R. Dickman and A. Yu. Tretyakov, cond-mat/9504050; J. F. F. Mendez and R. Dickman, *J. Phys. A* **27**, 3018 (1994); K. B. Lauritsen, F. Fröjd, and M. Howard, cond-mat/9808335; B. Tadić, *Phys. Rev. E* **59**, 1452 (1999).  
 [19] See W. Kleemann, *Int. J. Mod. Phys. B* **7**, 2469 (1993), and references therein.  
 [20] R. J. Birgeneau, R. A. Cowley, G. Shirane, H. Yoshizawa, D. P. Belanger, A. R. King, and V. Jaccarino, *Phys. Rev. B* **27**, 6747 (1983).  
 [21] A. Omerzu *et al.* (unpublished).